Supporting Information

Yang et al. 10.1073/pnas.1206081109

SI Materials and Methods

Proteins and Reagents. Biotinylated RecBCD enzymes with RecC-channel mutations were purified from an *Escherichia coli* strain harboring four plasmids, pMS421 (*lacI*^{q} spc) (1), pPB700 [(2) (*recB*, amp)], derivatives of pNH336 harboring the RecC-channel mutations (*recC*-channel mutants, cam) (3), and pWKS6 [biotin-*recD* kan; a derivative of pWKS130 (4)] in a Δ*recBCD* background. Cells for producing biotinylated RecBCD enzymes were grown in L broth with selective antibiotics and biotin (113 μM). After addition of 1 mM isopropyl-beta-D-thiogalactopyranoside at an OD_{600} of 0.5–0.6, cells were grown for 3–4 h and then harvested. RecC-channel mutants were purified as previously described (5) up to the Q-Sepharose chromatography step. After dialysis against 0.1 M potassium phosphate (pH 7.2) and 0.15 M NaCl, the pool from the Q-Sepharose column (Amersham-Pharmacia) was applied to an UltraLink Immobilized Monomeric Avidin column (Pierce). Biotinylated RecBCD was eluted with 2 mM D-biotin (Sigma), dialyzed to remove biotin, and then stored in 20 mM Tris-HCl (pH 7.5), 0.1 mM EDTA, 0.1 mM DTT, 100 mM NaCl, and 50% (vol/vol) glycerol (6). The concentrations of the purified RecC-channel mutants were determined using an extinction coefficient of 4.0×10^5 $M^{-1}{\cdot}cm^{-1}$ at 280 nm (7). The specific activity of each mutant enzyme was based on helicase units (7), and appropriate concentrations of wild-type and mutant enzymes were used in each assay to provide equivalent amounts of DNA unwinding activity. RecBC was expressed without pWKS6 in a Δ*recBCD* background and purified (8). Wild-type RecBCD was purified as described previously (5). *E. coli* SSB and RecA proteins were purified as previously described (9, 10).

Chemicals were of reagent grade. Pyruvate kinase, phosphoenolpyruvate, and ATP were purchased from Sigma. Restriction endonucleases, shrimp alkaline phosphatase, T4 polynucleotide kinase were from New England Biolabs; [γ-^{32}P]ATP was from Perkin-Elmer; YOYO-1 was from Molecular Probes Inc. ATP was dissolved as concentrated stock solution at pH 7.5, and its concentration was determined spectrophotometrically using an extinction coefficient of 1.54×10^4 $M^{-1}{\cdot}cm^{-1}$ at 260 nm.

DNA Substrates. The NdeI-linearized pBR322 $\chi^{(+)-3F3H}$ (χ^3) (11) substrate has three tandem χ sequences at either end of the linear double-strand (dsDNA) in the proper orientation for RecBCD enzyme entering from that end. Plasmids pNH92, pNH868, pNH869, pNH1556, pNH870, pNH871, pNH872, pNH873, pNH874, pNH875, pNH94, and pNH95, are pBR322 derivatives containing either χ or a variant χ sequence (12), flanked by BamHI and HindIII sites (Table S1). Plasmid DNA was linearized with NdeI or AvaI, and radioactively labeled at the 5′ end by reaction with shrimp alkaline phosphatase, and then with T4 polynucleotide kinase and [γ-^{32}P] ATP. Excess [γ-^{32}P] ATP was removed using a G-25 or S-200 spin column (GE Healthcare). The dsDNA concentration (nucleotides) was determined using a molar extinction coefficient of 6,290 $M^{-1}{\cdot}cm^{-1}$ at 260 nm.

DNA Unwinding Assay. Assays were performed as described previously (7, 13). The reaction mixtures contained 25 mM Tris acetate (pH 7.5), 2 magnesium acetate, 1 mM DTT, 10 μM (nucleotides) linear pBR322 dsDNA ^{32}P-labeled at the 5′-ends (2.25 nM ends), 1 mM ATP, and 2 μM SSB protein. DNA unwinding reactions were started with the addition of 0.1 nM RecBCD, 10 nM RecBC, or equivalent (in terms of helicase units) concentrations of RecC-channel mutants (0.5 nM Q38A, 0.3 nM T40A, 0.2 nM L64A, 0.5 nM W70A, 0.3 nM D133A, 0.2 nM D136A, 0.4 nM Q137A, 0.5 nM R142A, 0.4 nM R186A, 0.4 nM R186H, 0.3 nM D705A, and 0.4 nM D705H), after preincubation of all other components at 37 °C for 5 min. Assays were stopped at the indicated times by addition of proteinase K to a concentration of 0.5 mg/mL, which was dissolved in 5× sample loading buffer [250 mM EDTA, 2.5% (wt/vol) SDS, and 0.25% (wt/vol) Bromophenol blue]. After a 5-min incubation with proteinase K at 37 °C the reaction products were separated on a 1% (wt/vol) TAE agarose gel at 600 V·h, visualized, and quantified using an Amersham Biosciences Storm 840 PhosphorImager and ImageQuant software.

χ-Specific Single-Stranded DNA Fragment Production Assay. Assays were performed as described previously (5, 14–16). The reaction mixtures contained 25 mM Tris acetate (pH 7.5), 1 mM DTT, 10 μM (nucleotides) linear NdeI-linearized or AvaI-linearized pBR322 dsDNA (χ^3, or a single variant-χ) that was ^{32}P-labeled at the 5′-ends (2.25 nM ends), 2 μM SSB protein, and the indicated concentrations of magnesium acetate and ATP. DNA unwinding reactions were started with the addition of 0.1 nM of RecBCD enzyme, 10 nM RecBC enzyme, or equivalent concentrations of RecC-channel mutants (same as for the DNA unwinding assays), after preincubation of all other components at 37 °C for 5 min. Reactions were stopped, loaded on a 1% (wt/vol) agarose and analyzed as described above for the DNA unwinding assay.

Joint Molecule Formation Assay. Coupled RecABCD reactions were performed as described previously (17). The reactions contained 25 mM Tris acetate (pH 7.5), 6 mM magnesium acetate, 2 mM ATP, 1 mM DTT, 1 mM phosphoenolpyruvate, 4 Units/mL pyruvate kinase, 2 μM SSB protein, and 10 μM (nucleotides) of NdeI-linearized, 5′-end-labeled dsDNA (χ^3). In addition, 20 μM (nucleotides) supercoiled pBR322 DNA and 5 μM RecA were included before preincubation at 37 °C. The reactions were initiated with 0.1 nM RecBCD, 10 nM RecBC or equivalent amounts of the RecC-channel mutants (same as for the DNA unwinding assays). Reactions were stopped, loaded on a 1% (wt/vol) agarose, and analyzed as described above for the DNA unwinding assay. The yield of joint molecules formation was determined from the percentage of discrete joint molecules produced relative to the input dsDNA.

Reversible Inactivation Assay. Assays were performed as described previously (14, 15, 18). Initial reaction conditions contained 25 mM Tris acetate (pH 7.5), 1 mM magnesium acetate, 5 mM ATP, 1 mM DTT, 6.25 μM plasmid DNA (χ^0 or χ^3, 1.55 nM dsDNA ends), and 1.25 μM SSB protein. After equilibration for 2 min at 37 °C, reactions were initiated by addition of 0.05 nM RecBCD or the equivalent amount of RecC-channel mutant enzyme, and time points were taken as indicated. After 40 min, magnesium acetate was added to 10 mM final concentration, and the time course was continued for an additional 40 min. Reactions were stopped, loaded on a 1% agarose, and analyzed as described above for the DNA unwinding assay. Quantification of duplex DNA remaining was normalized to the amount present at the start of the reaction.

Single-Molecule Visualization. The DNA bead preparations and reactions were performed as previously described (19–22). The *cosA* end of λ DNA was attached to beads via a biotinylated oligonucleotide (5′-GGGCGGCGACCT-biotin-3′) that was ligated to the λ DNA using modification of a procedure used

previously (19). The biotinylated DNA (1–5 femtomoles) was incubated with 1–2 μL of 1 μm ProActive streptavidin-coated microspheres (Bangs Laboratories) for 1 h at 37 °C in 80 mM $NaHCO_3$ (pH 8.2). Bead-DNA complexes were transferred into 0.5 mL of degassed sample solution containing 45 mM $NaHCO_3$ (pH 8.2), 20% (wt/vol) sucrose, 50 mM DTT, and 20 nM YOYO-1 dye (Molecular Probes). DNA was incubated with the dye for at least 1 h in the dark at room temperature. Immediately before transfer to the sample syringe, 2 mM magnesium acetate, 8 nM RecBCD enzyme, or 24 nM of RecBC(D705A)D mutant enzyme, were added to the sample mixture. The reaction solution contained 45 mM NaHCO3 (pH 8.2), 20% (wt/vol) sucrose, 50 mM DTT, 1 mM ATP, 2 mM magnesium acetate, and 20 nM YOYO-1 at 29 °C.

Videos of the enzyme translocation were recorded at 5.3 frames per second with Andor iQ (Andor) software. Every two frames were averaged using an ImageJ plug-in to reduce background and to create movies at 2.65 frames per second. The length of the DNA molecule in each frame was measured with a plug-in written in this laboratory (22). The unwinding rates are the best fit values for the slopes of DNA unwinding ± SE obtained from the regression analysis to a contiguous three-segment line using GraphPad Prism Software v4. Values for the extent of DNA unwinding are the difference between the initial length of the DNA molecule and its final length after unwinding. Rates before and after a pause are the best fit values for the slopes of DNA unwinding ± SE obtained from the regression analysis. The average extent of unwinding, n, is calculated as follows. The number of enzymes (Y) that unwound at least a given DNA length (grouped in 2-kb bins) was plotted against that length (X). Processivity, P, was determined by fitting the data to the equation $Y = A \times P^X$. The value of N was obtained from P by the equation $N = 1/(1 - P)$ (20). N is reported as the mean ± SE.

Values for the position of the pause are the average length of the DNA molecule measured for each video frame during the appropriate reaction stage ± SE for the DNA lengths measured during this stage. SE for each pause position was calculated using following formula: $SE\ of\ pause\ position = \sqrt{(SE\ of\ intercept1)^2 + (slope1 \times SE\ of\ t1)^2 + (t1 \times SE\ of\ slope1)^2}$, where $t1$ is the beginning of the pause, $intercept1$ is the intercept of the Y/DNA length axis with the unwinding segments before pausing, and $slope1$ is the unwinding rate before pause. The duration of the pause was calculated by subtracting the time when the pause began from the time when the pause ended. SE for the duration of each pause was calculated using following formula:

$SE\ of\ pause\ duration = \sqrt{(SE\ of\ t1)^2 + (SE\ of\ t2)^2}$, where $t1$ and $t2$ are the beginning and the end of the pause.

The sequence and position of single-base variants of χ (arrows in Fig. 5 *A* and *D*) in λ DNA, relative to the cosB entry site, are: *ACTGGTGG* (20,248 bp), G**A**TGGTGG (31,046 bp, 19,857 bp), G**G**TGGTGG (46,285 bp, 32,585 bp), *GC**A**GGTGG* (36,298 bp), GC**C**GGTGG (12,883 bp, 7,069 bp), *GCTG**A**TGG* (39,319 bp, 30783 bp, 15,596 bp, 11,158 bp), GCTG**T**TGG (20,870 bp, 20,764 bp), GCTG**C**TGG (12,035 bp), *GCTGG**A**GG* (5,877 bp, 1,516 bp), GCTGG**C**GG (21,405 bp, 21,141 bp, 20,116 bp, 17,362 bp, 1,559 bp), *GCTGGT**A**G* (45,696 bp), GCTGGT**T**G (42,857 bp, 40,948 bp, 12,832 bp), and *GCTGGTG**C*** (21,835 bp); the variants examined biochemically in Fig. 4 (green arrows in Fig. 5 *A* and *D*) are italicized.

1. Heath JD, Weinstock GM (1991) Tandem duplications of the lac region of the *Escherichia coli* chromosome. *Biochimie* 73:343–352.
2. Boehmer PE, Emmerson PT (1991) *Escherichia coli* RecBCD enzyme: Inducible overproduction and reconstitution of the ATP-dependent deoxyribonuclease from purified subunits. *Gene* 102:1–6.
3. Handa N, et al. (2012) Molecular determinants responsible for recognition of the single-stranded DNA regulatory sequence, χ, by RecBCD enzyme. *Proc Natl Acad USA*, 10.1073/pnas.1206076109.
4. Wang RF, Kushner SR (1991) Construction of versatile low-copy-number vectors for cloning, sequencing and gene expression in *Escherichia coli*. *Gene* 100:195–199.
5. Bianco PR, Kowalczykowski SC (1997) The recombination hotspot Chi is recognized by the translocating RecBCD enzyme as the single strand of DNA containing the sequence 5′-GCTGGTGG-3′. *Proc Natl Acad Sci USA* 94:6706–6711.
6. Handa N, Bianco PR, Baskin RJ, Kowalczykowski SC (2005) Direct visualization of RecBCD movement reveals cotranslocation of the RecD motor after χ recognition. *Mol Cell* 17:745–750.
7. Roman LJ, Kowalczykowski SC (1989) Characterization of the helicase activity of the *Escherichia coli* RecBCD enzyme using a novel helicase assay. *Biochemistry* 28: 2863–2873.
8. Dillingham MS, Spies M, Kowalczykowski SC (2003) RecBCD enzyme is a bipolar DNA helicase. *Nature* 423:893–897.
9. Mirshad JK, Kowalczykowski SC (2003) Biochemical characterization of a mutant RecA protein altered in DNA-binding loop 1. *Biochemistry* 42:5945–5954.
10. LeBowitz JH (1985) Biochemical mechanism of strand initiation in bacteriophage lambda DNA replication. PhD thesis (The Johns Hopkins Univ, Baltimore).
11. Anderson DG, Kowalczykowski SC (1997) The recombination hot spot χ is a regulatory element that switches the polarity of DNA degradation by the RecBCD enzyme. *Genes Dev* 11:571–581.
12. Arnold DA, Handa N, Kobayashi I, Kowalczykowski SC (2000) A novel, 11 nucleotide variant of χ, χ*: One of a class of sequences defining the *Escherichia coli* recombination hotspot χ. *J Mol Biol* 300:469–479.
13. Arnold DA, Bianco PR, Kowalczykowski SC (1998) The reduced levels of χ recognition exhibited by the $RecBC^{1004}D$ enzyme reflect its recombination defect in vivo. *J Biol Chem* 273:16476–16486.
14. Dixon DA, Kowalczykowski SC (1991) Homologous pairing in vitro stimulated by the recombination hotspot, Chi. *Cell* 66:361–371.
15. Dixon DA, Kowalczykowski SC (1993) The recombination hotspot χ is a regulatory sequence that acts by attenuating the nuclease activity of the *E. coli* RecBCD enzyme. *Cell* 73:87–96.
16. Spies M, Dillingham MS, Kowalczykowski SC (2005) Translocation by the RecB motor is an absolute requirement for χ-recognition and RecA protein loading by RecBCD enzyme. *J Biol Chem* 280:37078–37087.
17. Anderson DG, Kowalczykowski SC (1997) The translocating RecBCD enzyme stimulates recombination by directing RecA protein onto ssDNA in a χ-regulated manner. *Cell* 90:77–86.
18. Dixon DA, Churchill JJ, Kowalczykowski SC (1994) Reversible inactivation of the *Escherichia coli* RecBCD enzyme by the recombination hotspot χ in vitro: Evidence for functional inactivation or loss of the RecD subunit. *Proc Natl Acad Sci USA* 91:2980–2984.
19. Bianco PR, et al. (2001) Processive translocation and DNA unwinding by individual RecBCD enzyme molecules. *Nature* 409:374–378.
20. Spies M, Amitani I, Baskin RJ, Kowalczykowski SC (2007) RecBCD enzyme switches lead motor subunits in response to χ recognition. *Cell* 131:694–705.
21. Spies M, et al. (2003) A molecular throttle: The recombination hotspot χ controls DNA translocation by the RecBCD helicase. *Cell* 114:647–654.
22. Amitani I, Liu B, Dombrowski CC, Baskin RJ, Kowalczykowski SC (2010) Watching individual proteins acting on single molecules of DNA. *Methods Enzymol* 472: 261–291.

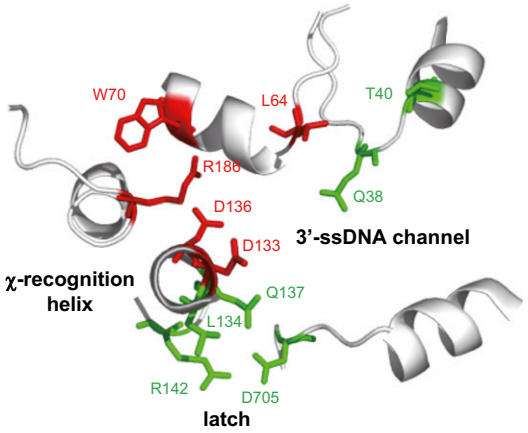

Fig. S1. Structural elements from the RecC channel showing the χ-recognition locus. Residues in red are lost-recognition; residues in green are relaxed-specificity. Regions of relevant secondary structure show χ-recognition helix, latch formed by R142 and D705, and the channel for the 3′-single-stranded DNA (ssDNA).

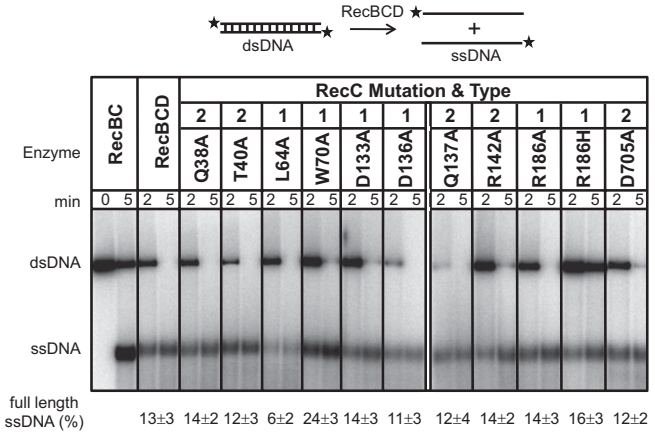

Fig. S2. All RecC-channel mutants retain helicase and nuclease activities that are comparable to wild-type. Time courses for dsDNA processing by RecBCD and mutant enzymes; the enzymes and reaction times are indicated. Reactions were carried out in the presence of 1 mM ATP and 2 mM $Mg(OAc)_2$, and the pBR322 dsDNA was linearized by NdeI. The positions of dsDNA and ssDNA species are indicated on the left. The final yields (± SD) of full-length ssDNA from at least three independent experiments are indicated under the gel; the normalized yield of full-length ssDNA for RecBC is 83 (±10)% and is an underestimate because of smearing of the ssDNA in the gel.

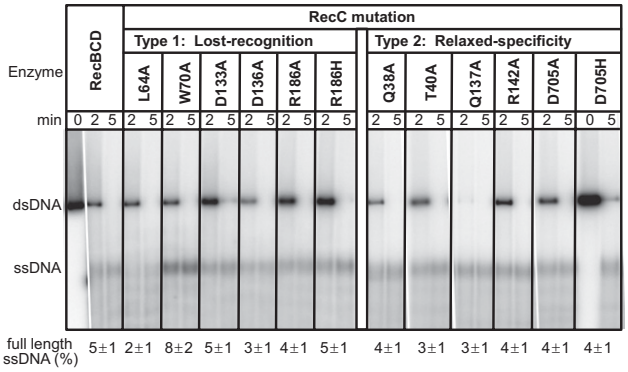

Fig. S3. At an elevated free Mg^{2+} concentration, the RecC-channel mutants display helicase and nuclease activities that, relative to one another, are comparable. Time courses for dsDNA processing by RecBCD and mutant enzymes; the enzymes and reactions times are indicated. Reactions were carried out in the presence of 2 mM ATP and 6 mM $Mg(OAc)_2$, and the pBR322 dsDNA was linearized by NdeI. Reactions from the same gel were rearranged in the order shown. The positions of dsDNA and ssDNA species are indicated on the left. The yields (± SD) of full-length ssDNA from at least three independent experiments are indicated under the gel.

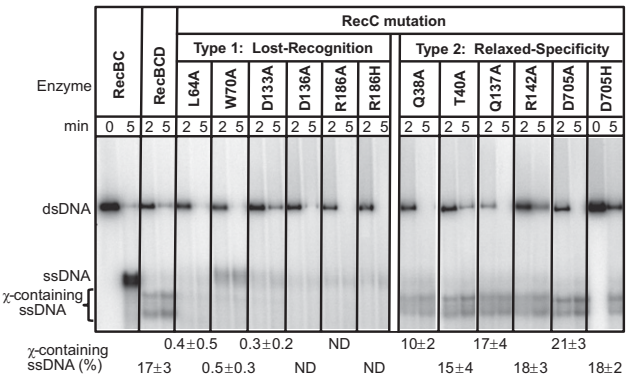

Fig. S4. At an elevated free Mg^{2+} concentration, the type 1 (lost-recognition) mutants process dsDNA to produce substantially reduced levels of χ-specific fragments; type 2 (relaxed-specificity) mutants display wild-type level of χ recognition. The production of χ-specific fragments was carried out using ^{32}P-labeled NdeI-linearized χ^3 dsDNA in the presence of 2 mM ATP and 6 mM $Mg(OAc)_2$. The enzymes and reactions times are indicated. The positions of substrate and products are depicted on the left. The yields (± SD) of χ-containing ssDNA from at least three independent experiments are indicated under the gel; ND signifies not detectable (<0.2%).

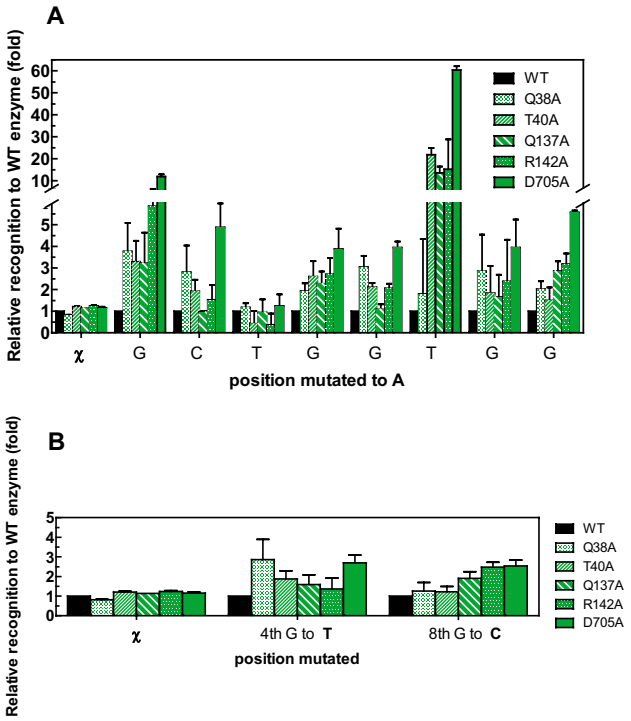

Fig. S5. Type 2 (relaxed-specificity) mutants recognize single-base variants of χ. The yield of variant χ-containing ssDNA produced by a mutant enzyme relative to that produced by the wild-type enzyme is plotted versus position of the canonical octameric χ sequence. Data are from Fig. 4; bars correspond to mutant enzyme described in the legend. (*A*) DNA substrates where each position of χ was replaced with an adenine residue ("A") mutation. (*B*) DNA substrates where the fourth or eighth positions of χ were replaced with thymine (T) or cytosine (C), respectively.

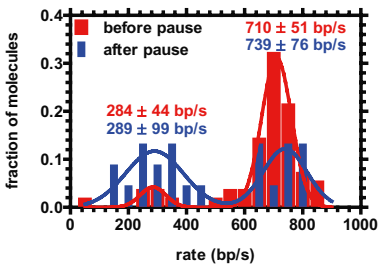

Fig. S6. Distribution of single-molecule translocation rates for RecBC(D705)D enzyme. The data were binned in 50-bp/s intervals and fit to the sum of two Gaussian distributions: the mean rates (± SD) for 56 molecules, before pausing, are: 284 ± 44 bp/s and 710 ± 51 bp/s; for the 23 that paused, the rates after the pause were 289 ± 99 bp/s and 739 ± 76 bp/s.

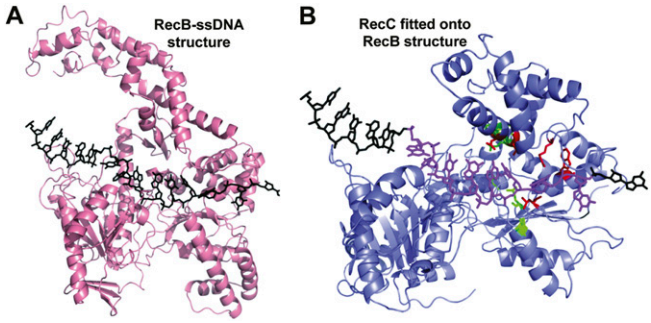

Fig. S7. Structural models for the interaction between χ and RecBCD (*A*) Ribbon diagram of the RecB subunit from RecBCD-DNA structure showing the location of the bound ssDNA. (*B*) Ribbon diagram of the RecC subunit with domains occupying the same positions as equivalent domains in RecB, and showing the proposed location of bound ssDNA. The eight bases in magenta are the χ sequence.

Table S1. List of plasmids containing a variant χ sequence

Plasmid	Sequence
pNH92	GCTGGTGG
pNH868	**A**CTGGTGG
pNH869	G**T**TGGTGG
pNH1556	G**A**TGGTGG
pNH870	GC**A**GGTGG
pNH871	GCT**A**GTGG
pNH872	GCT**T**GTGG
pNH873	GCTG**A**TGG
pNH874	GCTGG**A**GG
pNH875	GCTGGT**A**G
pNH94	GCTGGTG**C**
pNH95	GCTGGTG**A**

Boldface letters signify the variant. Plasmids pNH92, pNH94, and pNH95 were previously described (1); the others were constructed here as described in *SI Materials and Methods*.

1. Arnold DA, Handa N, Kobayashi I, Kowalczykowski SC (2000) A novel, 11 nucleotide variant of χ, χ*: One of a class of sequences defining the *Escherichia coli* recombination hotspot χ. *J Mol Biol* 300:469–479.

Table S2. Unwinding of λ DNA by RecBCD

Molecule	Unwinding rate (bp/s)	Extent of unwinding (bp)
1	374 ± 11	9,170
2	367 ± 19	5,830
3	794 ± 13	19,060
4	713 ± 10	27,470
5	286 ± 7	9,520
6	853 ± 6	40,480
7	802 ± 10	33,700
8	975 ± 16	16,120
9	854 ± 30	10,810
10	706 ± 20	13,040
11	781 ± 8	32,230
12	709 ± 26	11,540
13	584 ± 18	10,070
14	877 ± 14	21,430
15	248 ± 19	2,560
16	951 ± 8	34,800
17	883 ± 15	26,190
18	783 ± 8	36,630
19	859 ± 10	30,040
20	251 ± 12	7,140
21	794 ± 10	29,490
22	922 ± 23	14,410
23	479 ± 15	8,420
24	916 ± 8	37,630
Mean	368 ± 191	19,099 ± 868
	861 ± 99	

Reactions were performed in the presence of 1 mM ATP and 2 mM $Mg(OAc)_2$ at 29 °C. Unwinding rates are the best-fit values from linear regression analysis ± SE. Values for the mean rates were obtained by fitting the rate distribution to the sum of two Gaussian functions and are reported as the mean ± SD. The average extent of unwinding, *N*, is the mean ± SE.

Table S3. Unwinding of λ DNA by RecBC(D705A)D

Molecule	Rate before pause (bp/s)	Pause (s)	Rate after pause (bp/s)	Position of the pause (bp)	Extent of unwinding (bp)
1	714 ± 40	2.5 ± 2.7	140 ± 9	10,940 ± 830	11,560
2	783 ± 9	6.2 ± 0.5	784 ± 48	25,610 ± 420	28,910
3	724 ± 20	9.0 ± 0.4	744 ± 7	15,490 ± 560	40,080
4	710 ± 58	10.6 ± 0.6	658 ± 9	8,450 ± 890	28,300
5	849 ± 79	29.2 ± 0.5	811 ± 7	9,540 ± 1110	41,320
6	698 ± 104	4.9 ± 0.7	663 ± 4	6,880 ± 1290	41,030
7*	781 ± 5	5.7 ± 0.9	260 ± 7	35,810 ± 340	42,270
8	727 ± 13	2.2 ± 0.7	785 ± 17	20,200 ± 540	35,310
9	658 ± 24	21.4 ± 0.7	238 ± 7	11,190 ± 520	15,650
10	769 ± 21	6.2 ± 0.5	755 ± 15	16,020 ± 560	37,620
11	774 ± 9	4.0 ± 0.6	705 ± 43	25,020 ± 420	29,760
12	304 ± 3	12.6 ± 1.0	261 ± 7	20,830 ± 300	28,910
13	300 ± 14	3.3 ± 1.1	741 ± 6	8,110 ± 540	41,880
14	687 ± 25	6.7 ± 0.7	296 ± 4	12,190 ± 560	23,580
15*	684 ± 58	2.0 ± 0.9	327 ± 6	7,110 ± 780	17,530
16	247 ± 8	1.7 ± 1.7	675 ± 8	9,610 ± 530	37,970
17	683 ± 4	6.8 ± 0.7	460 ± 38	37,600 ± 340	38,840
18	269 ± 5	5.2 ± 0.8	412 ± 31	10,250 ± 260	13,800
19	607 ± 8	0.4 ± 2.0	323 ± 89	20,400 ± 590	21,020
20*	740 ± 23	1.6 ± 1.1	335 ± 8	13,840 ± 620	22,190
21	711 ± 9	4.3 ± 0.1	219 ± 20	23,830 ± 340	23,420
22	774 ± 6	1.3 ± 1.8	348 ± 107	22,550 ± 570	35,770
23	763 ± 9	1.0 ± 3.2	172 ± 4	35,490 ± 750	41,030
Mean	284 ± 44	4.2 ± 0.3	289 ± 99		23,206 ± 835
	710 ± 51		739 ± 76		

Reactions were performed in the presence of 1 mM ATP and 2 mM $Mg(OAc)_2$ at 29 °C. Unwinding rates before and after pausing are reported as the best fit values from three-segment line ± SE of the fitting. Values for the mean rates were obtained by fitting the rate distribution to the sum of two Gaussian functions and reported as the mean ± SD. The value for mean pause duration is the half-life time ± SE. The average extent of unwinding, *N*, was calculated from the extent of unwinding, as described in *SI Materials and Methods*, and is reported ± SE.
*Molecules depicted in Fig. 5*A*.